INFORMATICS JOURNALS

Research Article

Journal of Natural Remedies
DOI: 10.18311/jnr/2026/55608

eISSN: 2320-3358 | Vol 26(7), 2026 | pp. 1871-1890

Network Pharmacology and Molecular Simulation-based Exploration of Abietic Acid against Adenocarcinoma Targeting Hydrolase Enzymes

Nady Ghali[1] and Keval Raval[2*]

[1]Analytical Biochemist, P& P, London - EN48BU, England, United Kingdom

[2]Ramanbhai Patel College of Pharmacy, Charotar University of Science and Technology, CHARUSAT Campus, Changa, Anand – 388421, Gujarat, India; kevalraval.ph@charusat.ac.in

Abstract

Background: The protective potential of abietic acid against adenocarcinoma through targeting hydrolase enzymes was not explored, especially using network pharmacology and molecular simulations. **Aim:** To study the hydrolase enzymes mediated role of abietic acid against adenocarcinoma. **Methods:** The association of hydrolase enzymes with adenocarcinoma and abietic acid was initially established. A protein-protein interaction (PPI) network was constructed to identify significantly interacting proteins, which were further subjected to Gene Ontology (GO) and Kyoto Encyclopedia of Genes and Genomes (KEGG) enrichment analyses. A bioactive-target-pathway was constructed to characterise pathways involved with abietic acid. Gene expression patterns and survival of hydrolase enzymes in adenocarcinoma were analysed using TIMER 2.0. Molecular docking was performed to assess the binding interactions of abietic acid with PARP1, MMP9, and HDAC1. Molecular dynamics (MD) simulations were carried out for the unbounded state and the ligand-protein complex state of MMP to evaluate structural stability and binding stability. **Results:** Hydrolase enzymes, including PARP1, MMP9, and HDAC1, were identified as common targets of abietic acid and adenocarcinoma. GO and KEGG enrichment analyses revealed significant enrichment in adenocarcinoma related biological processes, cellular components, molecular functions, and signalling pathways. The bioactive target-pathway validated the association of abietic acid with adenocarcinoma-associated pathways. The gene expression and survival analysis indicated significant associations between hydrolase enzyme expression and decreased survival in adenocarcinoma subtypes. Molecular docking study indicated interactions of abietic acid with PARP1 (-9.4 kcal/mol), MMP9 (-9.4 kcal/mol), and HDAC1 (-9.7 kcal/mol). MD simulation study confirmed the dynamic stability of the abietic acid–MMP9 complex without a significant conformational disruption. **Conclusion:** Abietic acid demonstrated significant interactions with hydrolase enzymes and adenocarcinoma-associated pathways, suggesting the protective action against adenocarcinoma progression.

Major Findings: The study identified PARP1, MMP9, and HDAC1 as common hydrolase enzymes associated with adenocarcinoma. Furtherly, abietic acid demonstrated association with hydrolase enzymes, suggesting potential effect against adenocarcinoma.

Keywords: Abietic Acid, Adenocarcinoma, Hydrolase Enzymes, Molecular Dynamics Simulation, Network Pharmacology

(Article Chronicle: Article Received on: 30.03.2026; Revised on: 25.05.2026; Accepted on: 10.07.2026)

1. Introduction

Adenocarcinoma represents one of the most prevalent histological subtypes of cancer affecting organs such as the lung, breast, colon, prostate, pancreas, and stomach[1]. It is characterised by its metastatic potential and poor prognosis in advanced stages[2]. In 2025, adenocarcinoma constituted approximately 87% of the 226,650 new

*Author for correspondence

lung cancer cases and over 90% of the projected 67,440 pancreatic cancer cases[3]. The pathogenesis of adenocarcinoma involves molecular alterations, including activation of oncogenes[4], inactivation of tumour suppressor genes[5], and dysregulation of key signalling pathways, including MAPK/ERK[6], PI3K/AKT/mTOR[7], and Wnt/β-catenin[8]. These molecular disruptions promote emerging hallmarks of cancer, including uncontrolled cellular proliferation, resistance to apoptosis, sustained angiogenesis, and immune evasion[9].

Notably, the progression of adenocarcinoma involves dysregulation of certain hydrolase enzymes that promote malignant growth and spread[10]. Poly (ADPribose) polymerase 1 (PARP1), matrix metalloproteinase-9 (MMP-9), and histone deacetylase 1 (HDAC1) are among the key hydrolase enzymes that contribute to the progression of adenocarcinoma[11]. Overexpression of PARP1 facilitates DNA repair and tumour cell survival[12]. Similarly, MMP9 degrades the extracellular matrix to enable invasion and metastasis[13], and HDAC1 enforces epigenetic silencing of tumour suppressor genes, a change linked to more aggressive cancer phenotypes[14]. Hydrolase enzyme inhibitors hold therapeutic potential against adenocarcinoma by targeting dysregulated processes, including DNA repair[15], cell cycle control[16], epigenetic modification[17], matrix degradation[18], and apoptosis[19]. Current treatments like surgery, radiotherapy, and chemotherapy are effective for early-stage adenocarcinoma but are limited by metastasis, toxicity, and resistance[20]. Therefore, there is a compelling need for novel therapeutic strategies; this study addresses that gap by using a network pharmacology and molecular simulation approach to explore abietic acid as a multi-target agent against adenocarcinoma.

Abietic acid is a natural abietane diterpenoid resin acid predominantly found in the oleoresins of coniferous plants, especially species of *Pinus*, *Picea*, *Abies*, *Larix*, and *Cedrus*[21]. Abietic acid is reported to exhibit anti-inflammatory[22], anti-obesity[23], and anticonvulsant activities[24]. Recent studies suggest that abietic acid exhibits notable anticancer activity by promoting apoptosis[25], cell cycle arrest[26], and suppressing key oncogenic mediators such as NFκB, VEGF, and TGF-β1 to inhibit tumour proliferation, angiogenesis, and metastasis[27,28]. Given its polycyclic structure and pleiotropic bioactivity, abietic acid is hypothesised to interact with multiple key enzymes against adenocarcinoma. These characteristics provide a rationale to investigate abietic acid as a potential multi-target agent against adenocarcinoma.

In this study, it was postulated that abietic acid may inhibit the progression of adenocarcinoma by modulating the activity of the hydrolase enzymes. To test this hypothesis, the present study integrates network pharmacology with molecular modelling techniques to evaluate the potential of abietic acid to target hydrolase enzymes. Accordingly, the study was designed to validate the hydrolases as relevant targets in adenocarcinoma, followed by molecular docking and Molecular Dynamics (MD) simulations to characterise abietic acid's binding interactions with each enzyme. Additionally, network pharmacology analysis was employed to map the broader pharmacological networks and pathways influenced by abietic acid to explore the mechanistic insights of abietic acid against adenocarcinoma.

2. Materials and Methods

2.1 Target Validation

The association of target hydrolase enzymes (PARP1, MMP9, and HDAC1) with cancer was validated using the GeneCards® database (https://www.genecards.org/)[29]. A set of 100 topranked proteins associated with breast cancer, lung cancer, and colon cancer was retrieved based on relevance scores. Subsequently, the relationship of the selected targets with adenocarcinoma-associated proteins was intersected with abietic acid. The intersected proteins were considered a reference protein set and utilised for a network pharmacology study.

2.2 Network Pharmacology

2.2.1 Protein-Protein Interaction Network

A Protein–Protein Interaction (PPI) network was constructed for the reference protein set. The STRING database (version 11.5) was used to retrieve interactions[30]. The interaction confidence score was set to medium (≥0.4), and disconnected nodes were excluded for network clarity. The resulting interaction data were imported into Cytoscape (Version 3.9.1) for visualisation and further analysis[31]. Network topology

was assessed using the cytoHubba plugin, and degree centrality was employed to identify the 10 most significantly interacting proteins, which were ranked based on their degree of interaction.

2.2.2 Functional Enrichment Analysis

The most significantly interacting 10 proteins obtained from the PPI network were subjected to functional enrichment analysis. Gene Ontology (GO) pathways, including biological processes (BP), cellular components (CC), molecular functions (MF), and pathway enrichment based on the Kyoto Encyclopedia of Genes and Genomes (KEGG), were determined using DAVID Bioinformatics Resources (version 2021; https://david.ncifcrf.gov/)[32]. Gene symbols were used as input, and *Homo sapiens* was selected as the reference species. Significant enrichment was considered at a Benjamini-adjusted *P*-value < 0.05. Enriched KEGG pathways associated with the top targets were manually grouped into functional categories based on the degree of nodes.

2.2.3 Bioactive Target Pathway Interaction Network

A bioactive–target–pathway (BA–TAR–PATH) network was constructed using Cytoscape (Version 3.9.1; http://cytoscape.org)[33]. The most significantly interacting 10 proteins obtained from the PPI network were subjected to a two-layered interaction dataset generated by linking abietic acid to its protein targets, and targets to their associated KEGG pathways. The network was visualised with distinct node shapes and colours to differentiate the compound (triangle), target genes (squares), and pathways (ellipses), and arranged using a circular layout, placing abietic acid at the centre, surrounded by targets and outer pathways.

2.3 Expression Analysis

Gene expression analysis for the hydrolase enzymes was performed using TIMER 2.0 (http://timer.cistrome.org/) following the method by Zou *et al*[34]. Association between expression levels and clinical outcomes in the TCGA database comprising 10897 tumour samples across 32 different cancer types[35]. Additionally, the effect of high expression on the cumulative survival of cancer patients was investigated using TIMER 2.0, and Kaplan-Meier (KM) plots were generated.

2.4 Molecular Docking

2.4.1 Protein Preparation

Crystal structures of catalytic functional domains of PARP1 (PDB ID: 1a26)[36], MMP9 (PDB ID: 1gkc)[37], and HDAC1 (PDB ID: 1c3r)[38] were selected for the docking study. Water molecules were removed from proteins using the protein preparation wizard of Maestro 14.3, Schrodinger 2025[39]. Subsequently, the polar hydrogens were added, and grid areas were generated for each protein through the Schrodinger grid generator.

2.4.2 Ligand Preparation

A three-dimensional structure of abietic acid was prepared using ChemDraw 22.0.0 and Chem3D 22.0.0, and the structures were saved in PDB format[40].

2.4.3 Docking Procedure

The abietic acid structure was added to the Maestro workspace, and the best conformation was obtained through ligand preparation[41]. Subsequently, ligand compounds were subjected to energy minimisation, and the docking was initiated through the high-precision algorithm. The binding affinity for each compound was recorded, and the binding results for the docking and the compounds were visualised.

2.5 Molecular Dynamics

2.5.1 Apo Simulation

The Apo MD simulation was conducted following the standard procedure in the OpenMM simulation engine[42].

2.5.2 Force Field Selection

The ApoMD simulations for investigating the dynamics of MMP9 (PDB ID: 1gkc) in its unliganded state were conducted utilising the OpenMM simulation engine integrated with the AMBER force field parameters (ff14SB). The crystallographic structure of MMP9 was subjected to the removal of crystallographic water molecules, ions, and any bound ligands to represent the protein accurately in its Apo form.

2.5.3 Protein Preparation and Energy Minimisation

Initial preparation of the protein structure involved the AMBER LEaP module to generate parameters and topology files essential for simulations. The protein

structure was solvated in a truncated octahedral box using the TIP3P water model, maintaining a minimum distance of 12 Å between the protein surface and the simulation box edges to ensure adequate solvation and prevent boundary artefacts. Following system preparation, energy minimisation was performed using a sequential approach.

2.5.4 Equilibration and Production Simulation

Post-minimisation, equilibration was conducted employing the Langevin thermostat, and Monte Carlo barostatto stabilise the simulation system at a temperature of 26.85 ℃ and pressure of 1 atm. Production MD simulations were executed to monitor the structural dynamics of MMP9 for a 2ns trajectory at equilibrated temperature and pressure conditions.

2.6 Protein-ligand Simulation

The MD simulation of the protein-ligand complex was executed using the OpenMM simulation procedure[43].

2.6.1 Force Field Selection

The interaction between the ligand abietic acid and MMP9 (PDB ID: 1GKC) was examined through MD simulations performed using the OpenMM simulation engine integrated with AMBER force field parameters (ff14SB).

2.6.2 Ligand Preparation and Complex Generation

Ligand parameters for abietic acid were derived using the General Amber Force Field (GAFF). LEaP module of Ambertools was utilised to generate ligand topology and coordinate files. Abietic acid was docked into the active site of the protein to form an initial ligand-protein complex using molecular docking procedures. Subsequently, the assembled ligand-protein complex was solvated in a truncated octahedral box utilising the TIP3P water model, maintaining a 12 Å buffer between the protein-ligand complex and the box boundary to minimise boundary artefacts and ensure complete hydration. Post system assembly, the solvated ligand-protein complex underwent energy minimisation through restrained and unrestrained minimisations.

2.6.3 Production Simulation

Following successful equilibration, production-phase MD simulations were performed for 10 ns trajectory. and dynamic behaviour, structural fluctuations, and interaction patterns of abietic acid within the active site of MMP9 were studied.

2.7 Visualisation and Data Analysis

MD simulation trajectories were analysed using PyTraj, MDAnalysis, and ProLIF to evaluate the unbound and ligand-bound states of MMP9. Data analyses included assessments of conformational and interaction stability, secondary structural integrity, dynamic behaviour, and

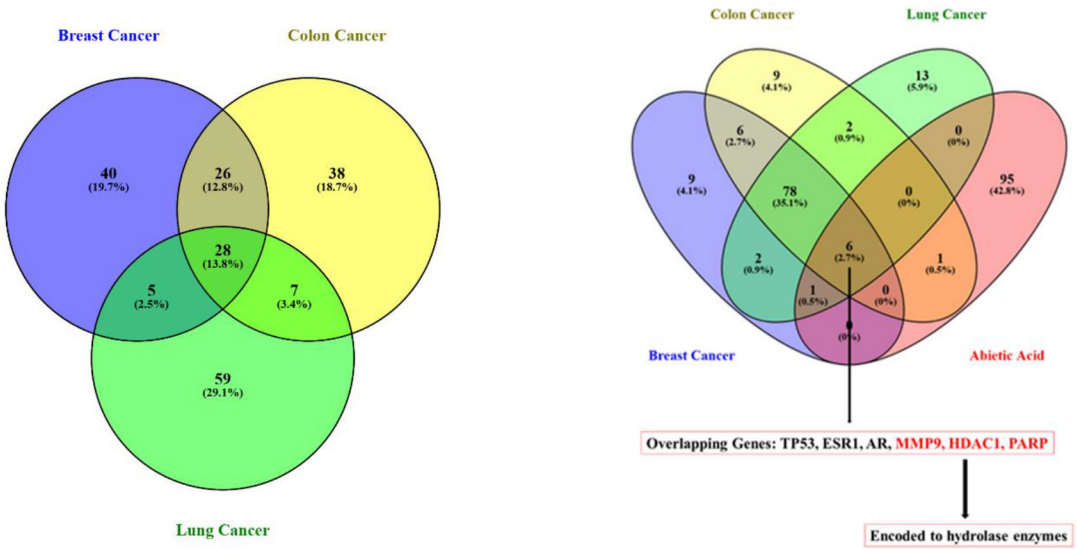


Figure 1. Cancer-associated proteins with abietic acid.

identification of transient binding sites. Quantitative metrics such as Root Mean Square Deviation (RMSD), Root Mean Square Fluctuation (RMSF), radius of gyration, hydrogen bond analysis, and principal component analysis (PCA) were employed to evaluate the structural dynamics of MMP9. Furthermore, detailed profiling of ligand-protein interactions, including hydrogen bonding, hydrophobic contacts, and electrostatic interactions, was conducted to elucidate the binding mechanism and stability of ligands within the MMP9 active site.

3. Results

3.1 Target Validation

Upon comparison with proteins associated with abietic acid, the reference protein set was observed across all three cancer types, including TP53, ESR1, AR, MMP9, HDAC1, and PARP1 (Figure 1). Among these, MMP9, HDAC1, and PARP1 are categorised as hydrolase enzymes.

3.2 Network Pharmacology

3.2.1 Protein-Protein Interactions

A total of 100 interacting proteins with the reference protein set were identified, and the top 10 proteins are presented in Figure 2. PARP2 demonstrated the strongest interaction with the reference protein set, followed by XRCC5, SIRT1, PARP14, MACROH2A1, PARP10, SIRT6, PARP2, XRCC1, and H2BC21.

3.2.2 Functional Enrichment Analysis

Figure 3 illustrates the GO pathway analysis of the most significantly interacting proteins. The BP analysis exhibited enrichment of processes, including the protein poly/auto-ADP-ribosylation, positive regulation of cytochrome c release from mitochondria, response to gamma radiation, p53 class mediator, negative regulation of fibroblast proliferation, doublestrand break repair, cellular response to UV, and intrinsic apoptotic signalling pathway. The CC analysis demonstrated enrichment in components, including the site of DNA damage, transcription repressor complex, site of double-strand break, transcription regulator complex, nuclear body, protein-containing complex, chromatin, nucleolus, nucleoplasm, and nucleus. The MF analysis highlighted the involvement of interacting proteins in activities, including protein lysine deacetylase, glutamate ADP-ribosyltransferase, nucleotidyltransferase, and NFkB binding.

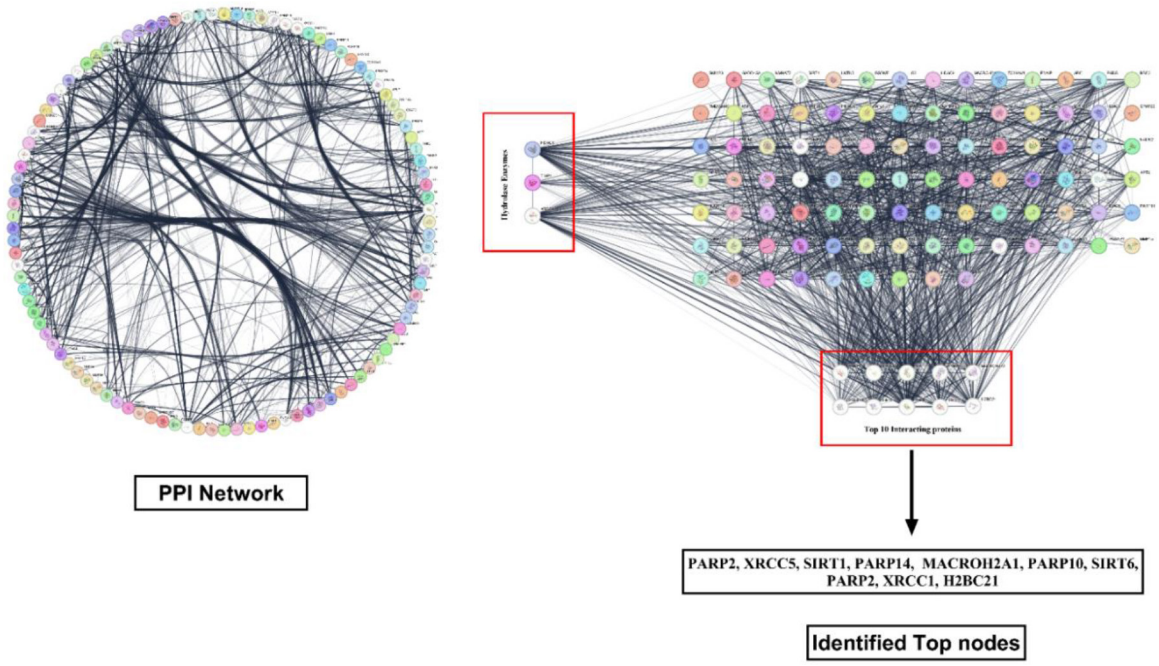


Figure 2. Protein-Protein Interaction (PPI) network and identified significantly interacting proteins with reference protein set.

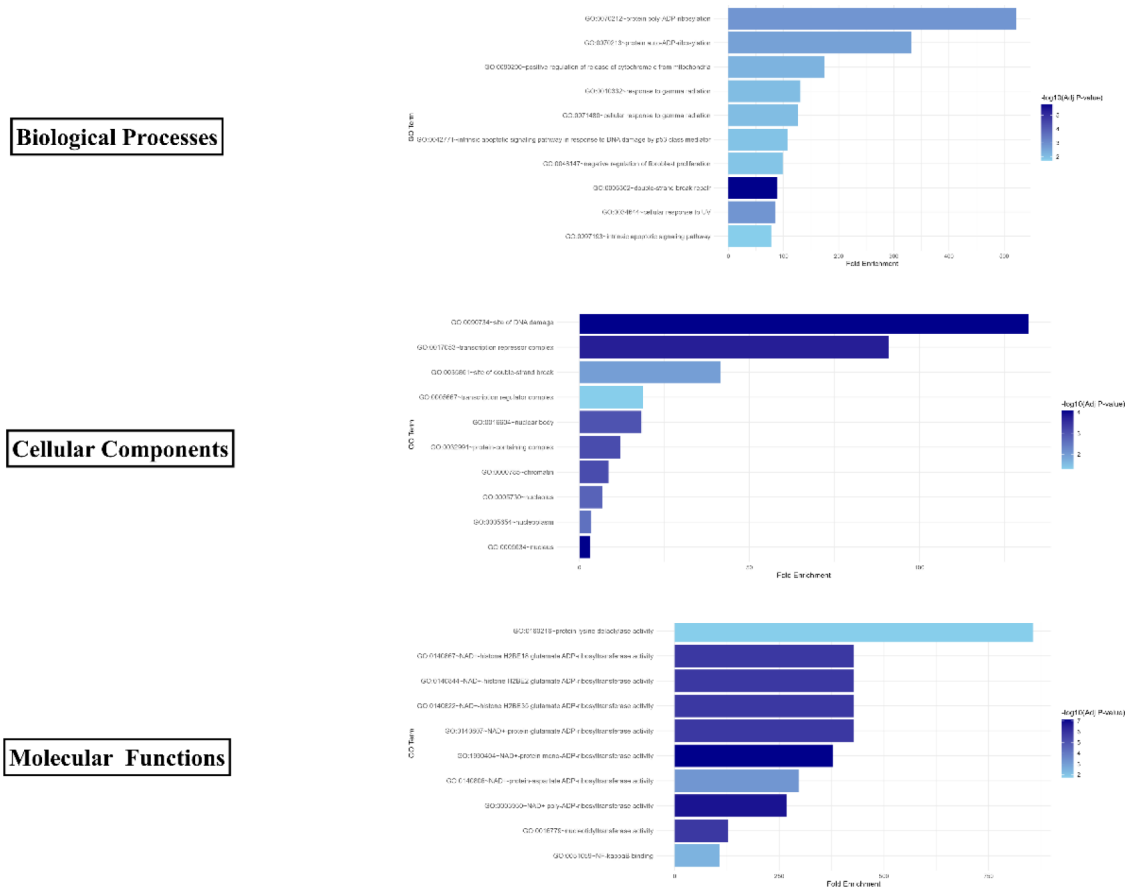


Figure 3. Graphical presentation of Gene Ontology Analysis highlighting 10 significantly enriched biological processes, cellular components, and molecular functions.

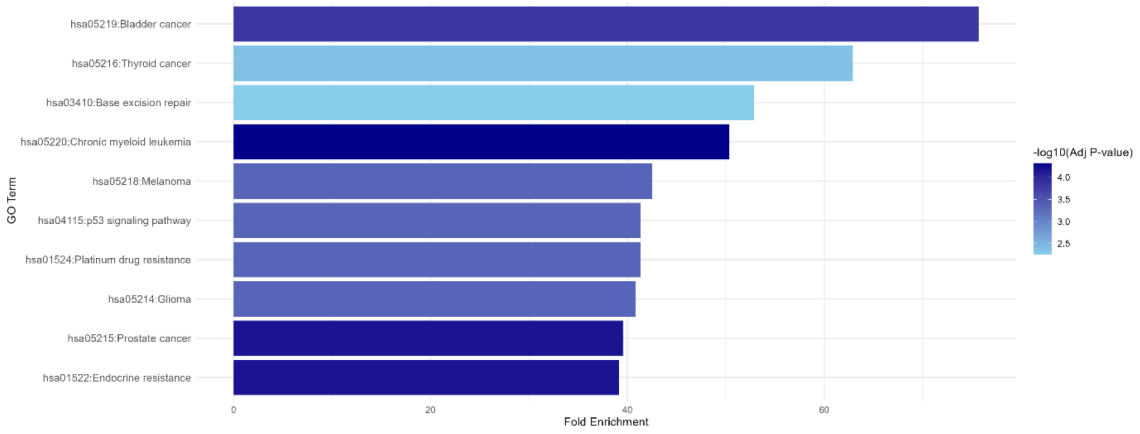


Figure 4. Graphical presentation of Kyoto Encyclopedia of Gene and Genome Analysis, highlighting 10 significantly enriched signalling pathways.

The KEGG pathway analysis demonstrated the involvement of interacting proteins in bladder cancer, thyroid cancer, base excision repair, chronic myeloid leukaemia, melanoma, p53 signalling pathway, platinum drug resistance, glioma, prostate cancer, and endocrine resistance (Figure 4).

Topological analysis of the target–pathway network using degree centrality revealed key hub genes such as

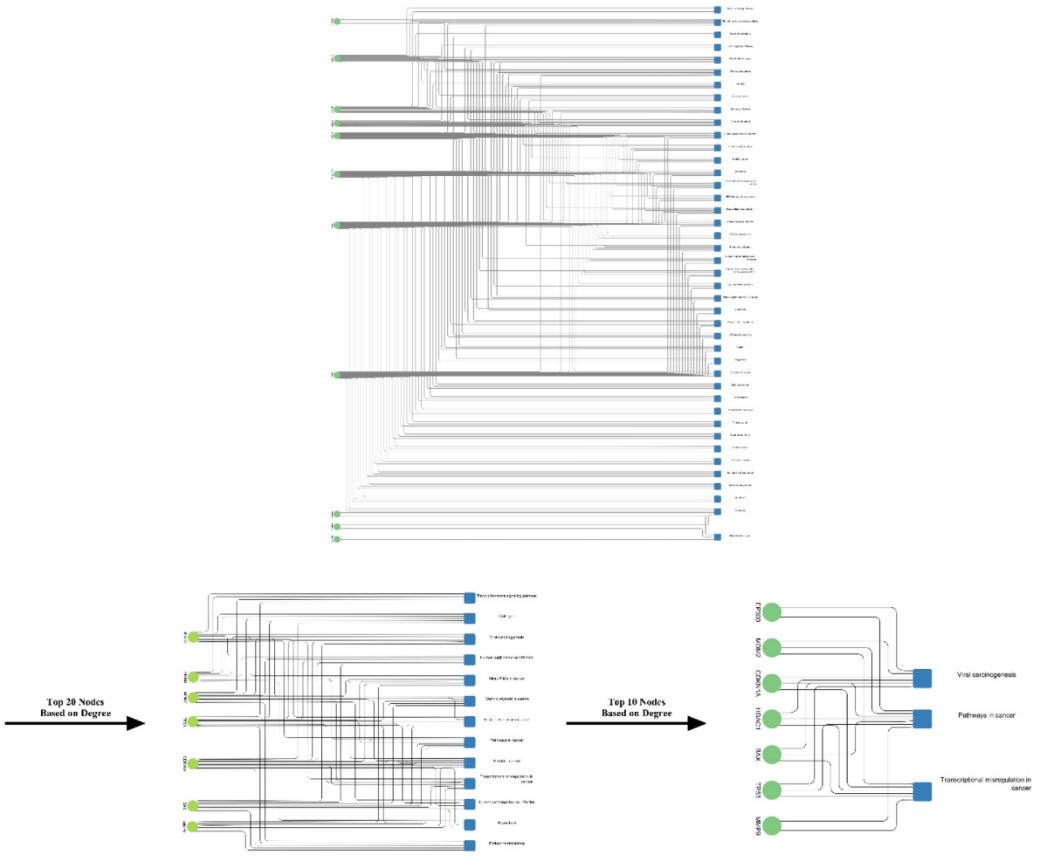


Figure 5. KEGG pathway categorisation based on high-degree target genes.

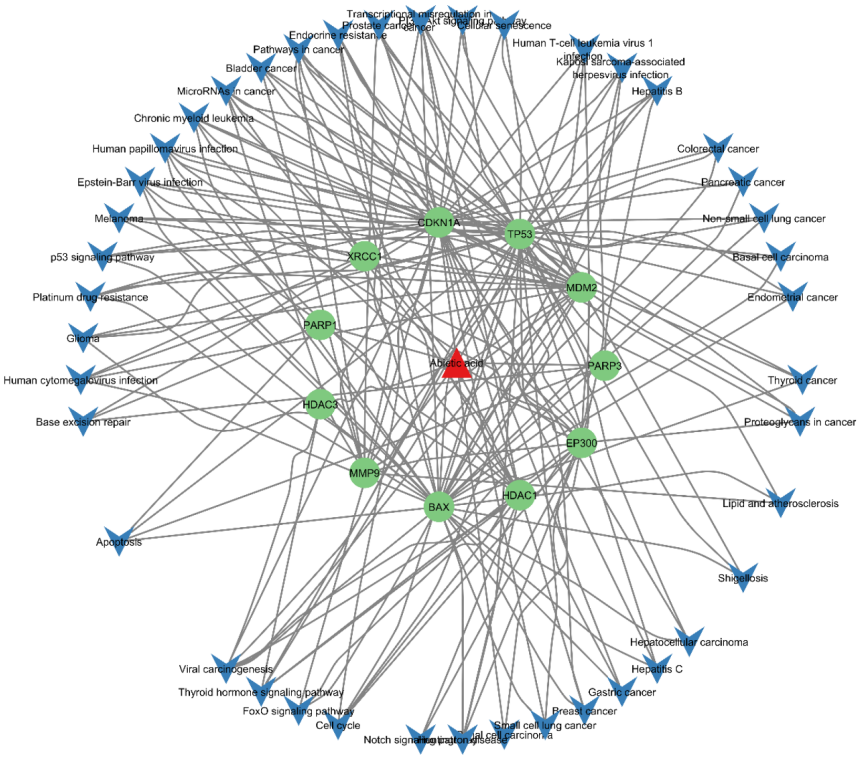


Figure 6. Bioactive–Target–Pathway (BA–TAR–PATH) interaction network of abietic acid.

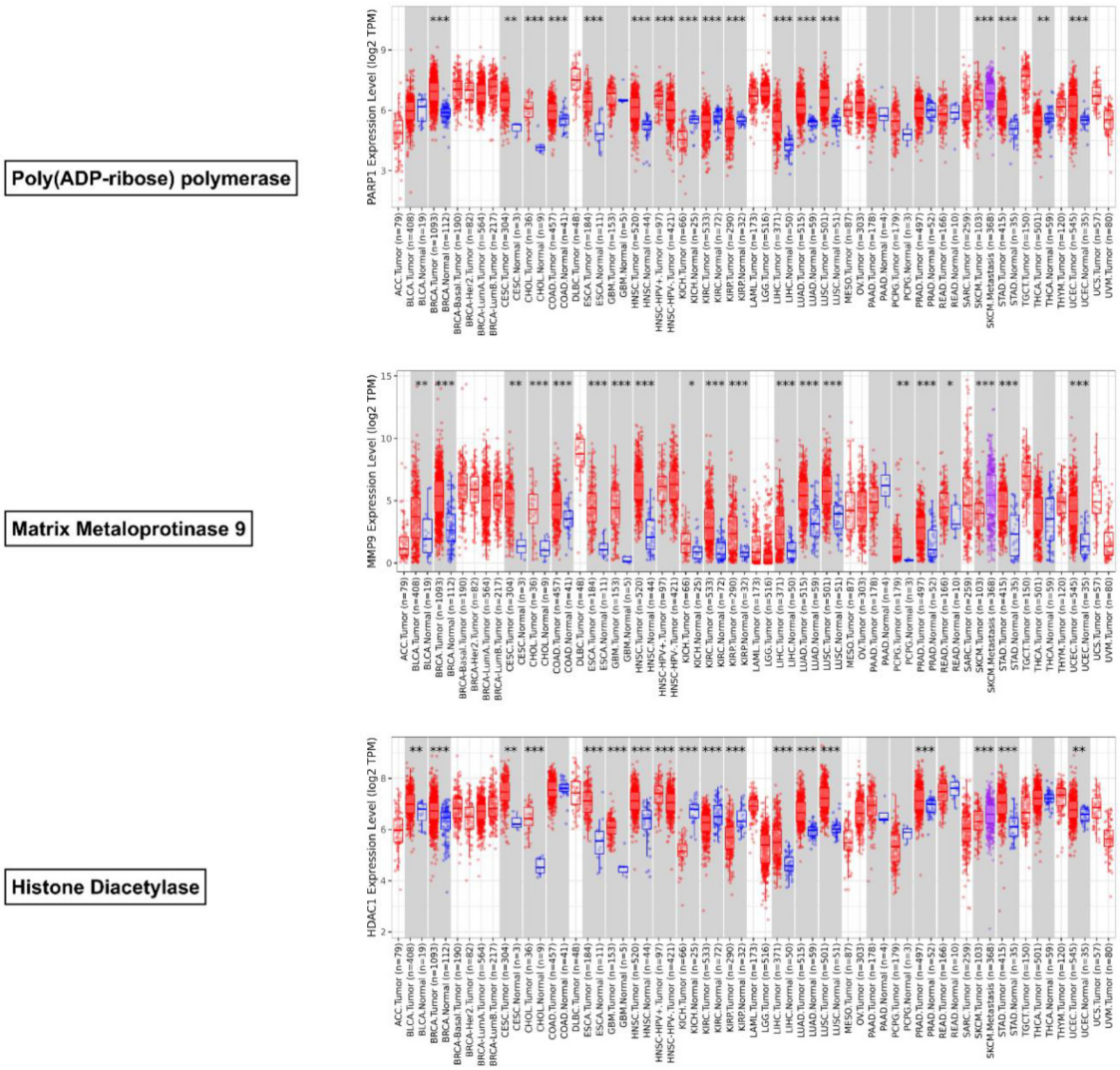


Figure 7. Comparative expression levels of hydrolase enzymes across breast, lung, and colon cancer tissues compared to normal controls (Symbols *, ** and *** indicate statistically significant differences in tumour tissues (red box) compared to normal tissues (blue box) with P-value < 0.05, P-value < 0.01 and Pvalue < 0.001, respectively).

TP53, CDKN1A, HDAC1, and MDM2, which exhibited the highest interaction density within the network (Figure 5). Subsequent KEGG pathway enrichment of these highdegree targets yielded a refined set of biologically relevant pathways.

3.2.3 BA-TAR-PATH Network

Notably, hub targets, including TP53, CDKN1A, PARP1, HDAC1, and MMP9, were observed to interact with multiple cancer-associated pathways, including apoptosis, p53 signalling, viral carcinogenesis, and chemical carcinogenesis. The BA-TAR-PATH network is illustrated in Figure 6.

3.3 Expression Analysis

Gene expression profiling from the TIMER 2.0 database revealed differential expression patterns of the three selected hydrolase enzymes across BRCA, LUAD, and COAD cancer types. PARP1 was significantly upregulated in BRCA (n = 1093), LUAD (n = 515), and COAD (n = 457) tumour tissues compared to their respective normal controls, with a P-value < 0.001 in all three datasets. MMP9 expression was significantly downregulated in BRCA (Pvalue < 0.001) and LUAD (P-value < 0.001), whereas COAD showed a non-significant expression difference between tumour and normal tissues. HDAC1 demonstrated

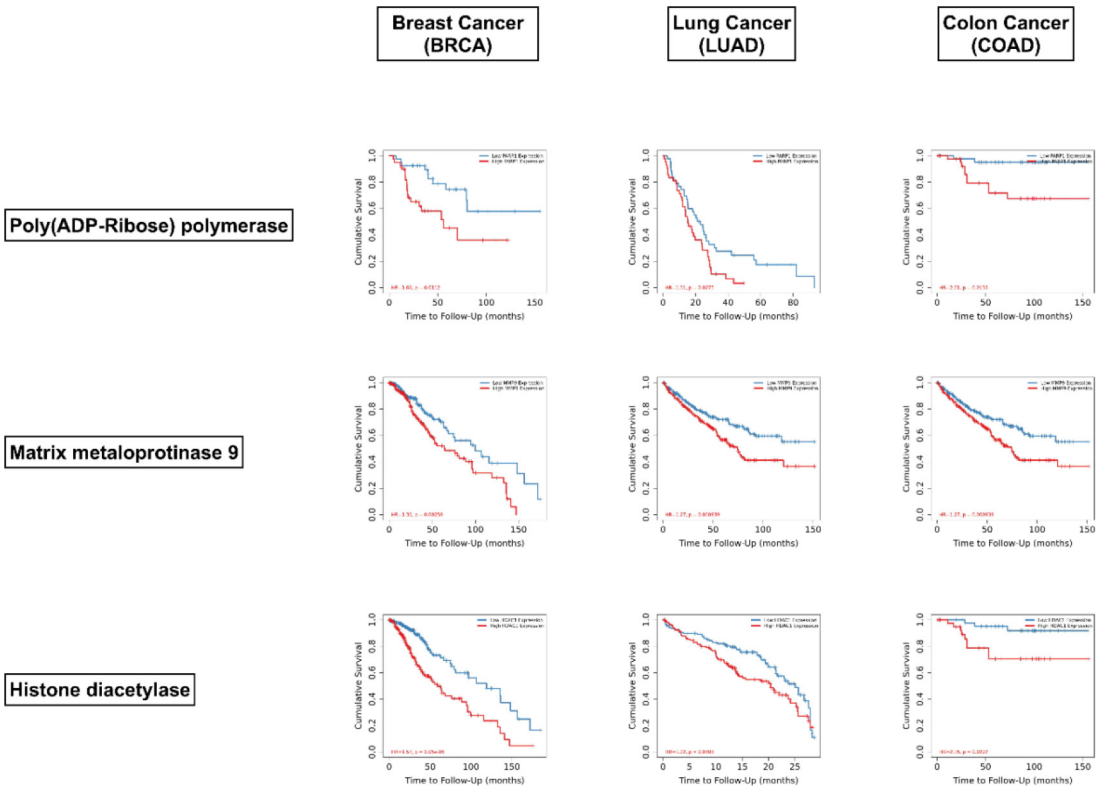


Figure 8. Impact of hydrolase enzyme expression on patient survival across breast, lung, and colon cancer datasets.

significant upregulation in BRCA (P-value < 0.001), LUAD (P-value < 0.001), and COAD (Pvalue < 0.001). Figure 7 illustrates the comparative expression levels of hydrolase enzymes across breast, lung, and colon cancer tissues compared to normal controls.

High expression of PARP1 was found to be associated with a significant reduction in cumulative survival across BRCA (HR = 1.42; P = 0.0072), LUAD (HR = 1.49; P = 0.012), and COAD (HR = 1.62; P = 0.0056). For MMP9, elevated expression correlated with poor survival in BRCA (HR = 1.23; P = 0.021), LUAD (HR = 1.27; P = 0.017), and COAD (HR = 1.31; P = 0.0042). HDAC1 upregulation was also linked with reduced survival probabilities in BRCA (HR = 1.33; P = 0.0013), LUAD (HR = 1.41; P = 0.0039), and COAD (HR = 1.52; P = 0.0021). three cancers. Figure 8 illustrates the impact of PARP1, MMP9, and HDAC1 expression on patient survival across breast, lung, and colon cancer datasets.

3.4 Molecular Docking

A tabular summary of molecular docking results is provided in Table 1. Abietic acid demonstrated a notable binding affinity with PARP1 (9.4 kcal/mol; 17 bonds), MMP9 (-9.4 kcal/mol; 20 bonds), and HDAC1 (-9.7 kcal/mol; 14 bonds). Abietic acid demonstrated binding interactions with PARP with charged bonds at ARG865, ARG878, LYS893, and ASP766, hydrogen bonds at SER864, ASN868, and GLN763, and hydrophobic interactions at TYR896, TYR889, ALA880, ILE879, ILE895, and TYR907. Additional bonds included van der Waals interactions with GLY894 and GLY863, polar bonds with HIS862 and HIS909, and a pi-cation interaction with ARG865. In MMP9, abietic acid exhibited hydrogen bonds with HIP131, HIS132, and HIE170, electrostatic bonds with ASP168, GLU92, and GLU195, π–π stacking with PHE141, PHE198, PHE200, TYR91, TYR296, and TYR297, and additional interactions with ASN20, HIE21, PRO22, GLY140, GLY295, LEU265, and PHE200. Against HDAC, abietic acid demonstrated a hydrogen bond with GLU402, polar bonds with HIS401, HIS405, and HIS411, a metal coordination bond with ZN1450, and hydrophobic interactions with TYR423, TYR420, VAL398, MET422, ALA189, LEU186-188, and PRO421, with additional contributions from

Table 1. Tabular summary of molecular docking results

Docking Score (kcal/mol)	Total Bonds	Interacting residues	Bond Category	Bond Type
Poly (ADP-ribose) polymerase 1 (PDB ID: 1A26)				
-9.4	17	ARG865, ARG878, LYS893	Charged (positive)	Distance
		ASP766	Charged (negative)	Distance
		SER864, ASN868, GLN763	Polar	Hydrogen bond
		TYR896, TYR889	Hydrophobic	Distance
		GLY894, GLY863	Glycine	Distance
		ALA880, ILE879, ILE895	Hydrophobic	Distance
		HIS862, HIS909	Polar	Distance
		TYR907	Hydrophobic	Distance
		Water	Water	Solvent exposure
		Ligand	-	Pi-cation (ARG865)
Matrix metaloprotienase-9 (1GKC)				
-9.4	20	HIP131, HIS132, HIE170	Polar/Charged	Hydrogen bond
		ASP168, GLU92, GLU195	Charged (negative)	Distance
		PHE141, PHE198, PHE200	Hydrophobic	Pi–Pi stacking
		TYR91, TYR296, TYR297	Hydrophobic	Pi–Pi stacking
		ASN20, HIE21, PRO22	Polar/Hydrophobic	Distance
		GLY140, GLY295	Glycine	Distance
		LEU265, PHE200	Hydrophobic	Distance
		Zn503	Metal	Metal coordination
Histone Deacetylase 1 (PDB ID: 1C3R)				
-9.7	14	GLU402	Charged (negative)	Hydrogen bond
		HIS401, HIS405, HIS411	Polar	Distance
		ZN1450	Metal	Metal coordination
		TYR423, TYR420	Hydrophobic	Distance
		VAL398, MET422	Hydrophobic	Distance
		ALA189, LEU186, LEU187, LEU188	Hydrophobic	Distance
		PRO421	Hydrophobic	Distance
		Water	Water	Solvent exposure

water-mediated bonds. Two-dimensional and three-dimensional interactions are presented in Figure 9.

3.5 Molecular Dynamics

3.5.1 Apo Simulation

The root mean square deviation (RMSD) analysis demonstrated a stabilised protein (~1.2 Å) with minor fluctuations observed throughout the simulation (Figure 10A). The corresponding distribution plot indicated a major population of conformations between 1.0 and 1.4 Å (Figure 10B). The 2D RMSD map displayed consistency in the structural transitions over the simulation period, with a diagonal dominance suggesting overall conformational stability (Figure 10C). The radius of gyration (Rg) remained relatively constant throughout the trajectory (13.4 Å and 13.8 Å, Figure 10D) and a compact conformation of the protein (Figure 10E). The probability distribution of Rg values further confirmed a narrow range of fluctuation (13.6 Å, Figure 10E). The dynamic cross-correlation matrix (DCCM) of Cα atoms revealed both positively

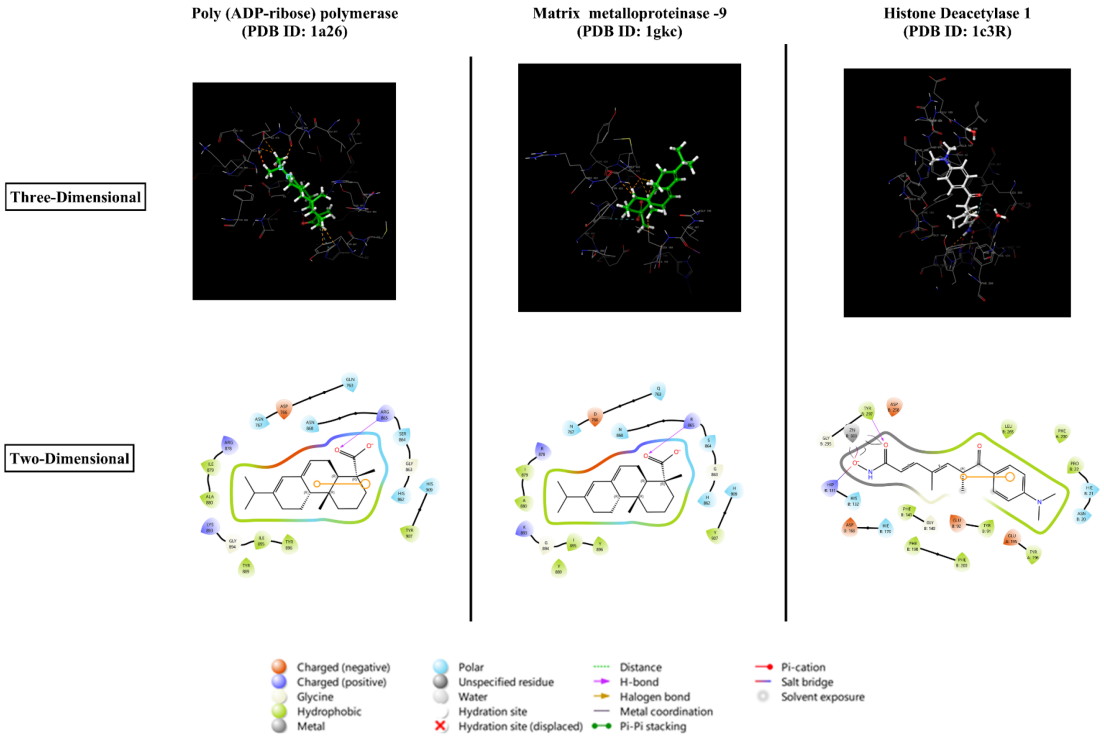


Figure 9. Graphical presentation of two-dimensional and three-dimensional interactions.

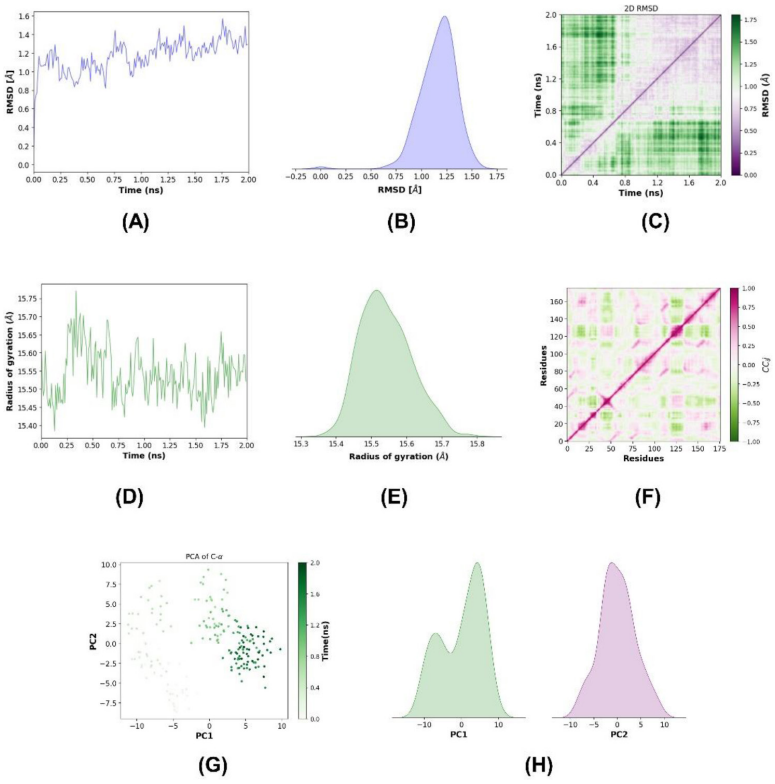


Figure 10. Molecular dynamics simulation analysis of the undocked protein over a 2 ns trajectory. **(A–B).** RMSD profile and distribution indicating overall structural stability; **(C).** 2D RMSD map showing conformational consistency; **(D–E).** Radius of gyration plot; **(F).** dynamic cross-correlation matrix of Cα atoms; **(G).** principal component analysis scatter plot of PC1 and PC2; **(H).** probability density distributions of PC1 and PC2.

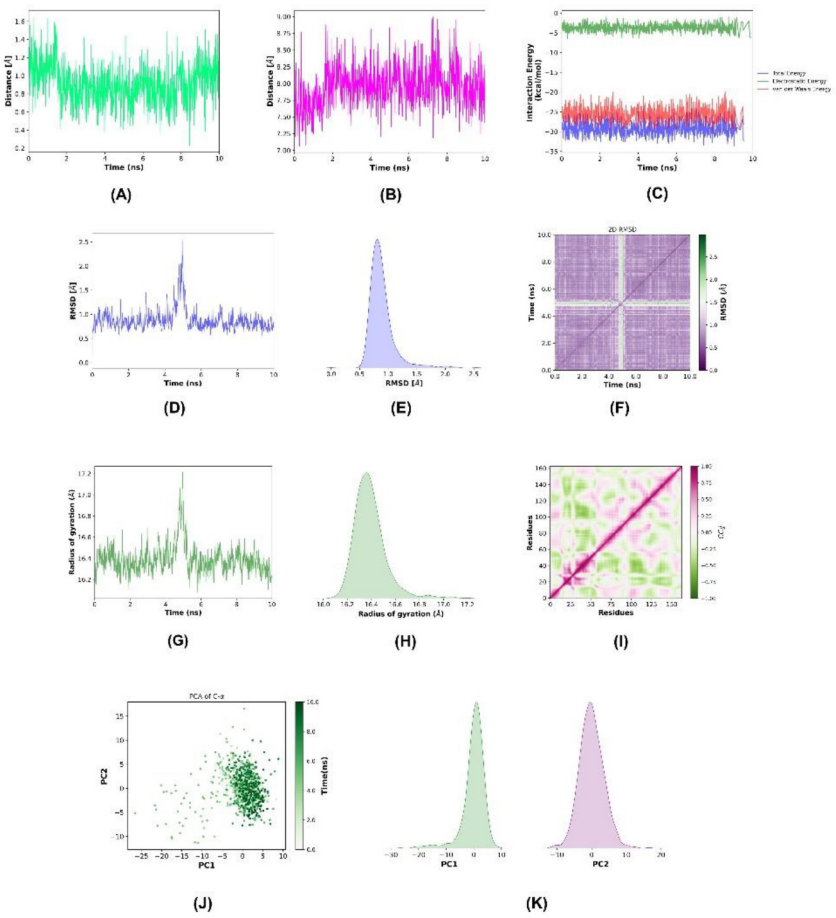


Figure 11. Molecular dynamics simulation analysis of the protein–ligand complex over a 10 ns trajectory. **(A–B).** Time evolution of distances between key protein–ligand atoms; **(C).** Total, potential, and kinetic energy profile; **(D–E).** RMSD plot and distribution with structural deviation patterns; **(F).** 2D RMSD map; **(G–I).** Radius of gyration plot and distribution; **(J).** Cross-correlation matrix of Cα atoms; **(K).** Principal component analysis scatter plot and eigenvalue distributions.

and negatively correlated motions among residues, with dominant intra-domain correlations shown along the diagonal (Figure 10F). The scatter plot of the first two principal components (PC1 and PC2) demonstrated a dispersed conformational sampling pattern (Figure 10G). The distribution of PC1 and PC2 values suggested heterogeneous movement within the sampled conformational space (Figure 10H).

3.5.2 Protein-ligand Simulation

Distance measurements between key interacting atoms remained relatively stable, with fluctuations between 7.0–8.5 Å and 6.5–9.0 Å (Figure 11 [A–B]). The total, kinetic, and potential energy profiles also remained consistent (Figure 11C). The RMSD of Cα atoms peaked at ~2.5 Å, with frequent fluctuations observed across the trajectory (Figure 11 [D-E]). The 2D RMSD map further confirmed temporal variations in structural conformations, with several deviations from the diagonal (Figure 11F). The Rg fluctuated moderately between 14.0–17.2 Å, with a dominant population around 15.2 Å (Figure 11 [G–H]). Dynamic crosscorrelation analysis revealed both correlated and anti-correlated motions among residues, with a predominant diagonal correlation pattern (Figure 11I). THE PCA revealed dispersion across the first two principal components (PC1 and PC2), indicating multiple conformational states sampled during the simulation (Figure 11 [J–K]).

4. Discussion

Hydrolase enzyme inhibitors have demonstrated therapeutic relevance in adenocarcinoma by disrupting epigenetic regulation, DNA repair, and extracellular matrix remodelling[44]. They are small-molecule inhibitors designed to fit into enzymatic active sites and disrupt catalytic function, thereby interfering with cancer-driving processes[45]. A recently developed novel class of compounds has been reported to simultaneously inhibit both PARP1 and HDAC, functioning through restoring BRCAlike homologous recombination deficiency and activating anti-tumour immune responses through the cGAS-STING pathway against triple-negative breast cancer[46]. A pre-clinical study highlighted the role of olaparib, vorinostat, and KT-3283 against Ewing sarcoma through simultaneously inhibiting PARP and HDAC[47]. Additionally, multiple studies have reported that HDAC inhibitors can downregulate MMP-9 expression to indirectly suppress tumour invasion and metastasis[48]. Although no single compound currently targets PARP1, MMP9, and HDAC1 concurrently, the observed downregulation of MMP9 via HDAC inhibition highlights a potential strategy for developing multi-target agents with tripartite efficacy in adenocarcinoma therapy.

Abietic acid has recently gained prominence for its emerging anticancer potential. Abietic acid is reported to prevent IκB phosphorylation and NF-κβ p65 nuclear translocation in non-small-cell lung cancer through the inhibition of IKKβ/NF-κβ signalling[49]. A study reported the inhibitory potential of abietic acid against PI3K/AKT signalling, which activates AMPK to induce apoptosis and autophagy in carcinomatous conditions[50]. Abietic acid is also reported to induce G_0/G_1 and G_2/M phase arrest to increase the expression of Fas, FasL, caspases-3/8, and cytochrome C in breast cancer cells[51]. A recent study evaluated the synergistic apoptotic effects of abietic acid with doxorubicin against colorectal cancer[52]. This study was conducted to examine the mechanistic insights into the anti-adenocarcinoma potential of abietic acid as a small-molecule inhibitor of hydrolase enzymes.

In this study, the target validation study was conducted to define a reference protein set for the network pharmacology analyses and to identify key hydrolase enzymes for subsequent gene expression profiling and molecular docking investigations. It confirmed the role of three hydrolase enzymes, PARP1, HDAC1, and MMP9, in adenocarcinoma. These hydrolase enzymes contribute to the progression of adenocarcinoma by promoting PARP1-mediated DNA repair[53], HDAC1-driven silencing of tumoursuppressor genes[54], and MMP9facilitated invasion and metastasis[55]. Network pharmacology analysis of the intersected proteins was conducted to elucidate the mechanistic relationship between hydrolase enzymes and abietic acid in adenocarcinoma. From the constructed PPI network, ten proteins were identified as significantly interacting with the reference protein set. Among these, six proteins, including PARP2[56], XRCC5[57], SIRT1[58], PARP14[59], PARP10[59], and SIRT6[60], have been reported in multiple studies to play tumorigenic roles in various cancers. The GO enrichment analysis revealed the significant association of several biological processes with adenocarcinoma, including DNA damage response[61], protein ADP-ribosylation[62], mitochondrial-mediated apoptosis[63], and cellular responses to genotoxic stress[64], which highlight the mechanistic involvement of interacted proteins in adenocarcinoma progression. Similarly, the GO enrichment analysis identified several nuclear-associated cellular components significantly linked to adenocarcinoma, including the site of DNA damage[65] and transcriptional regulators and repressor complexes[66]. These associations emphasise the functional involvement of the intersected proteins in genomic regulation and tumour progression within the nuclear environment[67]. The molecular functions GO analysis revealed the significant association of intersected proteins and adenocarcinoma, including protein lysine deacetylase activity[68], NAD - dependent ADP-ribosyltransferase activity targeting glutamate residues[69], and NF-κB binding[70], which collectively indicate the involvement of intersected proteins in epigenetic regulation and pro-survival signalling pathways in adenocarcinoma progression. Additionally, the KEGG pathway enrichment analysis revealed the significant involvement of several cancer-related signalling pathways in adenocarcinoma, including those associated with bladder and thyroid cancer[71], base excision repair[72], p53 signaling[73], platinum drug resistance[74], and endocrine resistance[75], indicating the potential role of the intersected proteins in tumorigenesis, genomic instability, and therapy

resistance. The subsequent network analysis validated the role of intersected proteins in viral carcinogenesis, transcriptional misregulation in cancer, and pathways in cancer. The bioactivetargetpathway network was constructed to connect the results from KEGG analysis with abietic acid, which validated the association of abietic acid with tumorigenic pathways.

Gene expression analysis revealed that PARP1, MMP9, and HDAC1 are significantly overexpressed in multiple cancer types, including lung, breast, and liver adenocarcinomas. Their elevated expression supports the functional association of hydrolase enzymes with aggressive malignancy[76] and poor long-term outcomes[77]. Survival analyses further demonstrated that high expression of PARP1, MMP9, and HDAC1 is associated with reduced overall survival in breast, lung, and colon adenocarcinomas. When integrated with genetic expression results showing their overexpression across these tumour types, these findings indicate their clinical relevance as prognostic biomarkers and therapeutic targets involved in epigenetic regulation[78]. This reinforces the importance of hydrolase enzymes and the ability of abietic acid to inhibit their activity, which may downregulate their downstream pro-cancer effects and sensitise cancer cells to apoptosis and growth arrest[79].

Moleculardockinganalysisprovideddetailedinsights into the binding behaviour of abietic acid with PARP1, MMP9, and HDAC1, revealing stable interactions at their respective catalytic domains. Notably, abietic acid exhibited charged, polar, and hydrophobic interactions with key residues of the NAD^+ binding site in PARP1, including ARG865, ARG878, and LYS893, crucial for catalysing DNA damage repair via ADP-ribosylation[80]. Furthermore, its pication interaction with ARG865 and multiple distance-based hydrogen and polar contacts mimic the binding interactions of established PARP inhibitors[80]. In MMP9, the carboxyl moiety of abietic acid demonstrated metal chelation in the active site of the protein, which resembles the interaction pattern of traditional hydroxamate inhibitors[81]. For HDAC, the carboxylic acid group of abietic acid demonstrated binding with the Zn^{2+} ion, which mimics the zinc-chelating mechanism of HDAC inhibitors such as vorinostat[82]. Additionally, interaction mapping showed strong hydrogen bonding with GLU401 and coordination with polar and hydrophobic residues, including TRP420, LEU156, and ALA189, collectively supporting stable accommodation in the HDAC1 catalytic pocket[83]. MMP9 was selected for molecular dynamics simulation based on its central involvement in adenocarcinoma- and abietic acid–related pathways, along with the strong zinc-chelating interaction observed in docking studies. The apo simulation was conducted for the MMP9 protein to establish the native conformational stability and dynamic behaviour of the unbound protein, which served as a baseline for comparing ligand-induced structural and functional changes[84]. The aposimulation of MMP9 demonstrated structural stability and limited conformational flexibility, which indicates its compact and catalically poised form of protein in the absence of ligands[85]. These findings establish a reliable dynamic baseline, supporting its suitability for comparative analysis with ligand-bound states, particularly in the context of zinc-chelating inhibitor interactions. The MD simulation of the abietic acid–MMP9 complex revealed a stable binding profile, which aligns with previous studies on zinc-chelating MMP inhibitors that maintain compact and rigid structural cores over simulation trajectories[86]. Radius of gyration analyses indicated preservation of protein folding of MMP9 upon ligand binding, contributing to the structural integrity of its zinc-dependent catalytic architecture[87]. Moreover, the principal component analysis demonstrated that abietic acid induced subtle conformational shifts rather than global unfolding, suggesting effective modulation without destabilising the protein[88].

However, the conclusions of this study rely on *in silico* studies, which require further validation through *in vitro* and *in vivo* investigations. *In vitro* cell-based models can be employed to explore the inhibitory potential of abietic acid against hydrolase enzymes. Additionally, cell viability studies, apoptosis assay, and migration assays can be conducted for abietic acid against adenocarcinoma. The anti-adenocarcinoma effect of abietic acid must be explored against chemically induced adenocarcinoma in experimental animals.

5. Conclusion

Three hydrolase enzymes, including PARP1, MMP9, and HDAC, were identified as functionally relevant in adenocarcinoma and were computationally

validated to interact with abietic acid. Subsequently, abietic acid-interacting proteins (including hydrolase enzymes) demonstrated significant interactions with tumorigenic proteins. The functional enrichment analysis revealed notable association of most significant tumorigenic proteins with biological processes, cellular components, and molecular functions and pathways related to adenocarcinoma. The bioactive-target-pathway network validated the association of abietic acid with adenocarcinoma-related molecular pathways. Furthermore, the molecular docking study demonstrated notable binding interactions of abietic acid with catalytic regions of PARP1, MMP9, and HDAC. The MD simulation revealed the stability of the MMP9 protein alone and in connection with abietic acid. *In vitro* biochemical inhibitory assays can be performed to confirm the multi-target inhibiting potential of abietic acid against target hydrolase enzymes. Additionally, investigations can be conducted to study the protective effect of abietic acid against adenocarcinoma in the biological system.

6. References

1. Ding H, Feng Y, Huang X, Xu J, Zhang T, Liang Y, Wang H, Chen B, Mao Q, Xia W, Huang X, Xu L, Dong G, Jiang F. Deep learning-based classification and spatial prognosis risk score on whole-slide images of lung adenocarcinoma. Histopathology. 2023; 83(2):211-228. https://doi.org/10.1111/his.14918 PMID: 37071058.
2. Travis WD, Brambilla E, Noguchi M, Nicholson AG, Geisinger KR, Yatabe Y, Beer DG, Powell CA, Riely GJ, Van Schil PE, Garg K, Austin JH, Asamura H, Rusch VW, Hirsch FR, Scagliotti G, Mitsudomi T, Huber RM, Ishikawa Y, Jett J, Sanchez-Cespedes M, Sculier JP, Takahashi T, Tsuboi M, Vansteenkiste J, Wistuba I, Yang PC, Aberle D, Brambilla C, Flieder D, Franklin W, Gazdar A, Gould M, Hasleton P, Henderson D, Johnson B, Johnson D, Kerr K, Kuriyama K, Lee JS, Miller VA, Petersen I, Roggli V, Rosell R, Saijo N, Thunnissen E, Tsao M, Yankelewitz D. International association for the study of lung cancer/american thoracic society/european respiratory society international multidisciplinary classification of lung adenocarcinoma. J Thorac Oncol. 2011; 6(2):244-285. https://doi.org/10.1097/JTO.0b013e318206a221 PMID: 21252716 PMCID: PMC4513953.
3. Siegel RL, Kratzer TB, Giaquinto AN, Sung H, Jemal A. Cancer statistics, 2025. CA Cancer J Clin. 2025; 75(1):10-45. https://doi.org/10.3322/caac.21871 PMID: 39817679 PMCID: PMC11745215.
4. Zuo X, Lei Y, Ou S, Yuan X, Shi P, Li Q, Xu Y. Integration of cuproptosis-related gene signatures in stomach adenocarcinoma: implications for prognostic prediction and therapeutic strategies in cancer drug resistance. Discov Oncol. 2025; 16(1):885. https://doi.org/10.1007/s12672-025-02740-8 PMID: 40410601 PMCID: PMC12102457.
5. Zuo S, Luo J, Liu M, Xu L, Dong J, Guo W, Zou S. Suppressing effects of down-regulating DNMT1 and DNMT3b expression on the growth of human cholangiocarcinoma cell line. J Huazhong Univ Sci Technolog Med Sci. 2008; 28(3):276-280. https://doi.org/10.1007/s11596-008-0310-7 PMID: 18563322.
6. Xu S, Xu Y, Chai W, Liu X, Li J, Sun L, Pan H, Yan M. KLRB1 expression is associated with lung adenocarcinoma prognosis and immune infiltration and regulates lung adenocarcinoma cell proliferation and metastasis through the MAPK/ERK pathway. J Thorac Dis. 2024; 16(6):3764-3781. https://doi.org/10.21037/jtd-24-8. Erratum in: J Thorac Dis. 2025; 17(2):1122-1125. https://doi.org/10.21037/jtd-2025b-01 PMID: 38983163 PMCID: PMC11228747.
7. Wang T, Seah S, Loh X, Chan CW, Hartman M, Goh BC, Lee SC. Simvastatin-induced breast cancer cell death and deactivation of PI3K/Akt and MAPK/ERK signalling are reversed by metabolic products of the mevalonate pathway. Oncotarget. 2016; 7(3):2532-2544. https://doi.org/10.18632/oncotarget.6304 PMID: 26565813 PMCID: PMC4823053.
8. Zhou S, Qian K, Yu S, Zhao Y, Shen Q, Li Y. MiR-4429 Alleviates malignant behaviors of lung adenocarcioma through Wnt/β-catenin pathway. Cancer Biother Radiopharm. 2024; 39(8):562-572. https://doi.org/10.1089/cbr.2021.0154 PMID: 34491827.
9. Hanahan D. Hallmarks of cancer: new dimensions. Cancer Discov. 2022; 12(1):31-46. https://doi.org/10.1158/2159-8290.CD-21-1059 PMID: 35022204.
10. Jaiswal S, Ayyannan SR. Anticancer potential of small-molecule inhibitors of fatty acid amide hydrolase and monoacylglycerol lipase. Chem Med Chem. 2021; 16(14):2172-2187. https://doi.org/10.1002/cmdc.202100120 PMID: 33834617.
11. Varier KM, Dan G, Liu W, Wu G, Xiao C, Lei H, Ling T, Jiang Y, Chen Y, Ben-David Y, Li Y, Zhang N, Gajendran B, Shen X. Stilbene B10 induces apoptosis and tumor suppression in lymphoid Raji cells by BTK-mediated regulation of the KRAS/HDAC1/EP300/PEBP1 axis. Biomed Pharmacother. 2022; 156:113887. https://doi.org/10.1016/j.biopha.2022.113887 PMID: 36274467.
12. Zhu C, Xu P, Li L, Wei H. Response to PARP inhibitor in EGFR-tyrosine kinase inhibitor-resistant metastatic lung adenocarcinoma with germline PALB2 mutation. Anticancer Drugs. 2025; 36(6):518-520. https://doi.org/10.1097/CAD.0000000000001712 PMID: 40029391.

13. Moro L, Arbini AA, Yao JL, di Sant'Agnese PA, Marra E, Greco M. Loss of BRCA2 promotes prostate cancer cell invasion through up-regulation of matrix metalloproteinase-9. Cancer Sci. 2008; 99(3):553-563. https://doi.org/10.1111/j.1349-7006.2007.00719.x Erratum in: Cancer Sci. 2014; 105(7):932. PMID: 18167127 PMCID: PMC11158040.
14. Rao L, Guo D, Wu JP. Cisplatin-resistance induces lung squamous carcinoma cell growth by nicotine-mediated α7nAchR/HDAC1/Cyclin D1/pRb cell cycle activation. Cell Biochem Funct. 2024; 42(2):e3990. https://doi.org/10.1002/cbf.3990 PMID: 38504444.
15. Wang X, Waldman L, Silberman Y, Wang M, Tackey C, Hanna L, Vesprini D, Emmenegger U, Eisen A, Smoragiewicz M. Mainstream model of genetic testing for prostate cancer at a large tertiary cancer centre. Clin Genitourin Cancer. 2024; 22(3):102052. https://doi.org/10.1016/j.clgc.2024.02.003 PMID: 38461085.
16. Yang D, Peng D, Zhou Y, Qiang Z, Wan L, Fan X, Meng Y, Xu G, Meng Y. Alpha-Momorcharin, a type I ribosome inactivating protein, induced apoptosis of hepatocellular carcinoma SK-HEP-1 cells through mitochondrial pathway. Nat Prod Res. 2025; 39(5):1128-1138. https://doi.org/10.1080/14786419.2023.2295915 PMID: 38126176.
17. Zand A, Macharia JM, Szabó I, Gerencsér G, Molnár Á, Raposa BL, Varjas T. The impact of tartrazine on DNA methylation, histone deacetylation, and genomic stability in human cell lines. Nutrients. 2025; 17(5):913. https://doi.org/10.3390/nu17050913 PMID: 40077783 PMCID: PMC11902176.
18. Yablecovitch D, Nadler M, Ben-Horin S, Picard O, Yavzori M, Fudim E, Duchan MT, Sakhnini E, Lang A, Lahav M, Saker T, Neuman S, Selinger L, Freitz B, Dvir R, Raitses-Gurevich M, Golan T, Levy I, Laish I. Serum matrix metalloproteinase-7, Syndecan-1, and CA 19-9 as a biomarker panel for diagnosis of pancreatic ductal adenocarcinoma. Cancer Med. 2024; 13(17):e70144. https://doi.org/10.1002/cam4.70144 PMID: 39263943 PMCID: PMC11391268.
19. Yi N, Zhang L, Huang X, Ma J, Gao J. Lenvatinib-activated NDUFA4L2/IL33/PADI4 pathway induces neutrophil extracellular traps that inhibit cuproptosis in hepatocellular carcinoma. Cell Oncol (Dordr). 2025; 48(2):487-504. https://doi.org/10.1007/s13402-024-01013-w PMID: 39585643 PMCID: PMC11996955.
20. Shi X, Wang X, Yao W, Shi D, Shao X, Lu Z, Chai Y, Song J, Tang W, Wang X. Mechanism insights and therapeutic intervention of tumor metastasis: latest developments and perspectives. Signal Transduct Target Ther. 2024; 9(1):192. https://doi.org/10.1038/s41392-024-01885-2 PMID: 39090094 PMCID: PMC11294630.
21. Hao M, Xu J, Wen H, Du J, Zhang S, Lv M, Xu H. Recent advances on biological activities and structural modifications of dehydroabietic acid. Toxins (Basel). 2022; 14(9):632. https://doi.org/10.3390/toxins14090632 PMID: 36136570 PMCID: PMC9501862.
22. Wahab NAA, Giribabu N, Kilari EK, Salleh N. Abietic acid ameliorates nephropathy progression via mitigating renal oxidative stress, inflammation, fibrosis and apoptosis in high fat diet and low dose streptozotocin-induced diabetic rats. Phytomedicine. 2022; 107:154464. https://doi.org/10.1016/j.phymed.2022.154464 PMID: 36215789.
23. Islam MT, Ali ES, Mubarak MS. Anti-obesity effect of plant diterpenes and their derivatives: a review. Phytother Res. 2020; 34(6):1216-1225. https://doi.org/10.1002/ptr.6602 PMID: 31977122.
24. Talevi A, Cravero MS, Castro EA, Bruno-Blanch LE. Discovery of anticonvulsant activity of abietic acid through application of linear discriminant analysis. Bioorg Med Chem Lett. 2007; 17(6):1684-1690. https://doi.org/10.1016/j.bmcl.2006.12.098 PMID: 17234417.
25. Ramnath MG, Thirugnanasampandan R, NagaSundaram N, Bhuvaneswari G. Molecular docking and dynamic simulation studies of terpenoids of *I. wightii* (Bentham) H. Hara against acetylcholinesterase and histone deacetylase3 receptors. Curr Comput Aided Drug Des. 2018; 14(3):234-245. https://doi.org/10.2174/1573409914666180321111925 PMID: 29564983.
26. Ren W, Liu T, Wu J. Unveiling abietic Acid's therapeutic potential: a narrative review on structure-activity relationship, pharmacological properties, pharmacokinetics, and toxicological considerations. Front Pharmacol. 2026; 16:1738572. https://doi.org/10.3389/fphar.2025.1738572. PMID: 41585866; PMCID: PMC12827616.
27. Thummuri D, Guntuku L, Challa VS, Ramavat RN, Naidu VGM. Abietic acid attenuates RANKL induced osteoclastogenesis and inflammation associated osteolysis by inhibiting the NF-KB and MAPK signaling. J Cell Physiol. 2018; 234(1):443-453. https://doi.org/10.1002/jcp.26575 PMID: 29932225.
28. Ahmad B, Tian C, Tang JX, Dumbuya JS, Li W, Lu J. Anticancer activities of natural abietic acid. Front Pharmacol. 2024; 15:1392203. https://doi.org/10.3389/fphar.2024.1392203 PMID: 38633616 PMCID: PMC11021724.
29. Liu Q, Luo Z, Sun M, Li W, Liu S. Mechanistic exploration and experimental validation of the *Xiaochaihu* decoction for the treatment of breast cancer by network pharmacology. Aging (Albany NY). 2024; 16(9):7979-7999. https://doi.org/10.18632/aging.205798 PMID: 38742934 PMCID: PMC11132012.
30. Zushuai M, Yanrong J, Chengdu Z, Xu Z, Qianshan D. Network pharmacological approach combined with weighted gene co-expression network analysis identifies CDKN2A as the keg target of *Changweiqing* against colorectal cancer. Hereditas. 2025; 162(1):33. https://doi.org/10.1186/s41065-025-00405-8 PMID: 40065477 PMCID: PMC11892207.
31. Zottel A, Šamec N, Jovčevska I. TNFSF14 and CD44 are overexpressed in glioblastoma and associated with

immunosuppressive microenvironment. Biomol Biomed. 2025; 25(8):1829-1843. https://doi.org/10.17305/bb.2025.11791. PMID: 39977830; PMCID: PMC12447739.
32. Zijie W, Anan J, Hongmei X, Xiaofan Y, Shaoru Z, Xinyue Q. Exploring the potential mechanism of *Fritillaria Irrhosae Bulbus* on ischemic stroke based on network pharmacology and experimental validation. Front Pharmacol. 2022; 13:1049586. https://doi.org/10.3389/fphar.2022.1049586 PMID: 36467049 PMCID: PMC9712457.
33. Jain NK, Tailang M, Chandrasekaran B, Khazaleh N, Thangavel N, Makeen HA, Albratty M, Najmi A, Alhazmi HA, Zoghebi K, Alagusundaram M, Jain HK. Integrating network pharmacology with molecular docking to rationalize the ethnomedicinal use of *Alchornea laxiflora* (Benth.) Pax and K. Hoffm. for efficient treatment of depression. Front Pharmacol. 2024; 15:1290398. https://doi.org/10.3389/fphar.2024.1290398 PMID: 38505421 PMCID: PMC10949534.
34. Zou H, Yin Y, Xiong K, Luo X, Sun Z, Mao B, Xie Q, Tan M, Kong R. Mitochondrial pyruvate carrier 1 as a novel prognostic biomarker in non-small cell lung cancer. Technol Cancer Res Treat. 2024; 23:15330338241282080. https://doi.org/10.1177/15330338241282080. PMID: 39360506 PMCID: PMC11452851.
35. Wang Z, Jensen MA, Zenklusen JC. A practical guide to The Cancer Genome Atlas (TCGA). Methods Mol Biol. 2016; 1418:111-1141. https://doi.org/10.1007/978-1-4939-3578-9_6 PMID: 27008012.
36. Wang Y, Bian F, Deng S, Shi Q, Ge M, Wang S, Zhang X, Xu S. The key residues of active sites on the catalytic fragment for paclitaxel interacting with poly (ADP-ribose) polymerase. J Biomol Struct Dyn. 2011; 28(6):881-893. https://doi.org/10.1080/07391102.2011.10508615 PMID: 21469749.
37. Binsuwaidan R, Elekhnawy E, Elseady WS, Keshk WA, Shoeib NA, Attallah NGM, Mokhtar FA, Abd El Hadi SR, Ahmed E, Magdeldin S, Negm WA. Antibacterial activity and wound healing potential of *Cycas thouarsii* R. Br n-butanol fraction in diabetic rats supported with phytochemical profiling. Biomed Pharmacother. 2022; 155:113763. https://doi.org/10.1016/j.biopha.2022.113763 PMID: 36182739.
38. Mostoufi A, Baghgoli R, Fereidoonnezhad M. Synthesis, cytotoxicity, apoptosis and molecular docking studies of novel phenylbutyrate derivatives as potential anticancer agents. Comput Biol Chem. 2019; 80:128-137. https://doi.org/10.1016/j.compbiolchem.2019.03.008 PMID: 30952039.
39. Younas S, Nosheen A, Malik ZI, Hussain N, Khan MU, Alhegaili AS, Shabbir Z, Manzoor S, Rehman HM, Hammad HM. Genetic analysis of HPV-16 L1 gene mutations and computational screening of therapeutic inhibitors for cervical cancer treatment. Med Oncol. 2025; 42(5):153. https://doi.org/10.1007/s12032-025-02711-7 PMID: 40192871.
40. Yang Z, Ji P, Li C, Wu F, Hua Y, Wei Y, Cao Y. Research progress on the chemical constituents and pharmacological effects of *Houttuynia cordata* Thunb and a predictive analysis of quality markers. Curr Issues Mol Biol. 2024; 47(1):18. https://doi.org/10.3390/cimb47010018 PMID: 39852133 PMCID: PMC11763989.
41. Tshilande N, Mammino L. Computable properties of selected monomeric acylphloroglucinols with anticancer and/or antimalarial activities and first-approximation docking study. J Mol Model. 2025; 31(4):113. https://doi.org/10.1007/s00894-025-06299-7 PMID: 40072710 PMCID: PMC11903629.
42. Zhou G, Liu X, Zhang S, Yu G, He H. A force field for molecular simulation of tetrabutylphosphonium amino acid ionic liquids. J Phys Chem B. 2007; 111(25):7078-7084. https://doi.org/10.1021/jp068365e PMID: 17552552.
43. Naveed M, Khatoon K, Aziz T, Naveed R, Majeed MN, Ud Din MS, Javed T, Khan AA, Alasmari AF. Scrutinizing the evidence of anthracene toxicity on adrenergic receptor beta-2 and its bioremediation by fungal manganese peroxidase via *in silico* approaches. Sci Rep. 2025; 15(1):3795. https://doi.org/10.1038/s41598-025-85889-0 PMID: 39885221 PMCID: PMC11782678.
44. Tripathy M, Bui A, Henderson J, Sun J, Woods CR, Somani S, Doan T, Louis Sam Titus ASC, Mohan C. FAAH inhibition ameliorates breast cancer in a murine model. Oncotarget. 2023; 14:910-918. https://doi.org/10.18632/oncotarget.28534 PMID: 37921652 PMCID: PMC10624203.
45. Zuo K, Qi Y, Yuan C, Jiang L, Xu P, Hu J, Huang M, Li J. Specifically targeting cancer proliferation and metastasis processes: the development of matriptase inhibitors. Cancer Metastasis Rev. 2019; 38(3):507-524. https://doi.org/10.1007/s10555-019-09802-8 PMID: 31471691.
46. Zhu Q, Dai Q, Zhao L, Zheng C, Li Q, Yuan Z, Li L, Xie Z, Qiu Z, Huang W, Liu G, Zu X, Chu B, Jiang Y. Novel dual inhibitors of PARP and HDAC induce intratumoral STING-mediated antitumor immunity in triple-negative breast cancer. Cell Death Dis. 2024; 15(1):10. https://doi.org/10.1038/s41419-023-06303-z PMID: 38182579 PMCID: PMC10770036.
47. Ramos L, Truong S, Zhai B, Joshi J, Ghaidi F, Lizardo MM, Shyp T, Kung SHY, Rezakhanlou AM, Oo HZ, Adomat H, Le Bihan S, Collins C, Bacha J, Brown D, Langlands J, Shen W, Lallous N, Sorensen PH, Daugaard M. A bifunctional PARP-HDAC inhibitor with activity in Ewing sarcoma. Clin Cancer Res. 2023; 29(17):3541-3553. https://doi.org/10.1158/1078-0432.CCR-22-3897 PMID: 37279093 PMCID: PMC10472104.
48. Hontecillas-Prieto L, Flores-Campos R, Silver A, de Álava E, Hajji N, García-Domínguez DJ. Synergistic enhancement

of cancer therapy using HDAC inhibitors: opportunity for clinical trials. Front Genet. 2020; 11:578011. https://doi.org/10.3389/fgene.2020.578011 PMID: 33024443 PMCID: PMC7516260.

49. Liu X, Chen W, Liu Q, Dai J. Abietic acid suppresses non-small-cell lung cancer cell growth via blocking IKKβ/NF-κB signaling. Onco Targets Ther. 2019; 12:4825-4837. https://doi.org/10.2147/OTT.S199161 PMID: 31354305 PMCID: PMC6590626.
50. Chen C, Gao H, Su X. Autophagy-related signaling pathways are involved in cancer (Review). Exp Ther Med. 2021; 22(1):710. https://doi.org/10.3892/etm.2021.10142 PMID: 34007319 PMCID: PMC8120650.
51. Haffez H, Osman S, Ebrahim HY, Hassan ZA. Growth inhibition and apoptotic effect of pine extract and abietic acid on MCF-7 breast cancer cells via alteration of multiple gene expressions using *in vitro* approach. Molecules. 2022; 27(1):293. https://doi.org/10.3390/molecules27010293 PMID: 35011526 PMCID: PMC8746537.
52. Haffez H, Sanad HH, Ebrahim H, Hassan ZA. Synergistic effects of abietic acid combined with doxorubicin on apoptosis induction in a human colorectal cancer cell line. Sci Rep. 2025; 15(1):16102. https://doi.org/10.1038/s41598-025-99616-2 PMID: 40341222 PMCID: PMC12062260.
53. Zhang Z, Sun C, Zhang L, Chi X, Ji J, Gao X, Wang Y, Zhao Z, Liu L, Cao X, Yang Y, Mao W. Triptolide interferes with XRCC1/PARP1-mediated DNA repair and confers sensitization of triple-negative breast cancer cells to cisplatin. Biomed Pharmacother. 2019; 109:1541-1546. https://doi.org/10.1016/j.biopha.2018.11.008 PMID: 30551406.
54. Xin L, Tan Y, Zhu Y, Cui X, Wang Q, Zhao J, Tian S, Xu C, Xiao M, Hong B, Xu J, Yuan X, Wang C, Kang C, Fang C. EPIC-0307-mediated selective disruption of PRADX-EZH2 interaction and enhancement of temozolomide sensitivity to glioblastoma via inhibiting DNA repair and MGMT. Neuro Oncol. 2023; 25(11):1976-1988. https://doi.org/10.1093/neuonc/noad102 PMID: 37279651 PMCID: PMC10628965.
55. Zong L, Cheng G, Zhao J, Zhuang X, Zheng Z, Liu Z, Song F. Inhibitory effect of ursolic acid on the migration and invasion of doxorubicin-resistant breast cancer. Molecules. 2022; 27(4):1282. https://doi.org/10.3390/molecules27041282 PMID: 35209071 PMCID: PMC8879026.
56. Khalid AB, Fountzilas C, Burney HN, Mamdani H, Schneider BP, Fausel C, Perkins SM, Jalal S. A phase II study evaluating safety and efficacy of niraparib in patients with previously treated homologous recombination defective metastatic esophageal/gastroesophageal junction/proximal gastric adenocarcinoma. Front Oncol. 2024; 14:1435056. https://doi.org/10.3389/fonc.2024.1435056 PMID: 39640282 PMCID: PMC11618106.
57. Ling S, Yu J, Zhan Q, Gao M, Liu P, Wu Y, Zhang L, Shan Q, Liu H, Wang J, Cai S, Zhou W, Que Q, Wang S, Hong J, Xiang J, Xu S, Liu J, Peng X, Wang N, Wang W, Xie H, Cai J, Wang L, Zheng S, Xu X. Multi-omic analysis reveals a CAF-stemness-governed classification in HCC liver transplant recipients beyond the Milan criteria. Nat Commun. 2025; 16(1):4392. https://doi.org/10.1038/s41467-025-59745-8 PMID: 40355422 PMCID: PMC12069600.
58. Zhao YS, Shi YK, Li KF, Ma B, Lin SH, Xing Y, Xu F. Dexmedetomidine regulates macrophage phenotype remodeling through AMPK/SIRT1 to alleviate inflammatory mediators and lung injury. J Biochem Mol Toxicol. 2025; 39(1):e70108. https://doi.org/10.1002/jbt.70108 PMID: 39692360.
59. Zhu Z, Weng S, Zheng F, Zhao Q, Xu Y, Wu J. Identification of Poly(ADP-ribose) polymerase 9 (PARP9) as a potent suppressor for *Mycobacterium tuberculosis* infection. Phenomics. 2023; 4(2):158-170. https://doi.org/10.1007/s43657-023-00112-2 PMID: 38884060 PMCID: PMC11169154.
60. Zhou HZ, Zeng HQ, Yuan D, Ren JH, Cheng ST, Yu HB, Ren F, Wang Q, Qin YP, Huang AL, Chen J. NQO1 potentiates apoptosis evasion and upregulates XIAP via inhibiting proteasome-mediated degradation SIRT6 in hepatocellular carcinoma. Cell Commun Signal. 2019; 17(1):168. https://doi.org/10.1186/s12964-019-0491-7 PMID: 31842909 PMCID: PMC6915971.
61. Żwierełło W, Maruszewska A, Nowak R, Kostrzewa-Nowak D, Tarasiuk J. DNA damage induced by NADPH cytochrome P450 reductase-activated idarubicin in sensitive and multidrug resistant MCF7 breast cancer cells. Pharmacol Rep. 2017; 69(1):185-195. https://doi.org/10.1016/j.pharep.2016.10.002 PMID: 27940401.
62. Sun C, Yao H, Liu J, Wang S. The effect of downregulation of ARL9 expression on the proliferation, metastasis and biological behavior of AGS gastric cancer cell lines. Adv Clin Exp Med. 2025; 34(8):1375-1382. https://doi.org/10.17219/acem/193399 PMID: 39776316.
63. Pajaniradje S, Subramanian S, Mohankumar K, Ronsard L, Anaikutti P, Rajagopalan R. A naturally derived glycosylated oleanolic acid derivative suppresses NF-κB translocation and induces intrinsic apoptosis in lung adenocarcinoma cells. Chem Biol Drug Des. 2025; 105(6):e70137. https://doi.org/111/cbdd.70137 PMID: 40468424.
64. Zhang Z, Li Y, Shi R, Jia C, Xu S, Zhu G, Cao P, Huang H, Li X, Zhang H, Liu M, Chen C, Liu H, Kang C, Chen J. L3MBTL1, a polycomb protein, promotes Osimertinib acquired resistance through epigenetic regulation of DNA damage response in lung adenocarcinoma. Cell Death Dis. 2024; 15(9):649. https://doi.org/10.1038/s41419-024-06796-2 PMID: 39231972 PMCID: PMC11374981.
65. Moosavi F, Hassani B, Nazari S, Saso L, Firuzi O. Targeting DNA damage response in pancreatic ductal adenocarcinoma: A review of preclinical and clinical evidence. Biochim Biophys Acta Rev Cancer. 2024; 1879(6):189185. https://

doi.org/10.1016/j.bbcan.2024.189185. Epub 2024 Sep 24. PMID: 39326802.

66. Huang X, Chen C, Chen Y, Zhou H, Chen Y, Huang Z, Xie Y, Liu B, Guo Y, Yang Z, Chen G, Su W. Silencing of the long non-coding RNA LINC00265 triggers autophagy and apoptosis in lung cancer by reducing protein stability of SIN3A oncogene. Oncol Res. 2024; 32(7):1185-1195. https://doi.org/10.32604/or.2023.030771. Erratum in: Oncol Res. 2025; 33(5):1249-1250. https://doi.org/10.32604/or.2024.061822 PMID: 38948024 PMCID: PMC11211643.
67. Fritz AJ, El Dika M, Toor RH, Rodriguez PD, Foley SJ, Ullah R, Nie D, Banerjee B, Lohese D, Tracy KM, Glass KC, Frietze S, Ghule PN, Heath JL, Imbalzano AN, van Wijnen A, Gordon J, Lian JB, Stein JL, Stein GS. Epigenetic-mediated regulation of gene expression for biological control and cancer: cell and tissue structure, function, and phenotype. Results Probl Cell Differ. 2022; 70:339-373. https://doi.org/10.1007/978-3-031-06573-6_12 PMID: 36348114 PMCID: PMC9753575.
68. Xu T, Fang Y, Gu Y, Xu D, Hu T, Yu T, Xu YY, Shen HY, Ma P, Shu Y. HDAC inhibitor SAHA enhances antitumor immunity via the HDAC1/JAK1/FGL1 axis in lung adenocarcinoma. J Immunother Cancer. 2024; 12(10):e010077. https://doi.org/10.1136/jitc-2024-010077 PMID: 39384195 PMCID: PMC11474878.
69. Shetti P, Kashid V, Wankhede N, Parameswaran S. Synthesis of fluoro and nitro pyrazoline derivatives: anticancer and molecular docking studies. Chempluschem. 2025; 90(6):e202500024. https://doi.org/10.1002/cplu.202500024 PMID: 40052369.
70. Zhou H, Wu Y, Meng J, Zhao X, Hou Y, Wang Q, Liu Y. C1QBP modulates DNA damage response and radiosensitivity in hepatocellular carcinoma by regulating NF-κB activity. Int J Mol Sci. 2025; 26(10):4513. https://doi.org/10.3390/ijms26104513 PMID: 40429658 PMCID: PMC12111173.
71. Xiong X, Zeng L, Zeng F, Huang Y, Jia L. Bioinformatics exploration of the S1PR1 receptor in various human cancers and its clinical relevance. Discov Oncol. 2025; 16(1):449. https://doi.org/10.1007/s12672-025-02241-8 PMID: 40172754 PMCID: PMC11965076.
72. Zuckerman JT, Jackson AS, Minko IG, Kant M, Jaruga P, Stone MP, Dizdaroglu M, McCullough AK, Lloyd RS. Functional characterization of single nucleotide polymorphic variants of DNA repair enzyme NEIL1 in South Asian populations. DNA Repair (Amst). 2024; 139:103695. https://doi.org/10.1016/j.dnarep.2024.103695 PMID: 38795603 PMCID: PMC11218669.
73. Zhang L, Wang S, Wang L. SKA1/2/3 is a prognostic and predictive biomarker in esophageal adenocarcinoma and squamous cell carcinoma. BMC Cancer. 2024; 24(1):1480. https://doi.org/10.1186/s12885-024-13257-8 PMID: 39614199 PMCID: PMC11607974.
74. Zhao L, Han H, Zhou X, Gong T, Zhu Y, Xiao B, Liu S, Zhao W, Wu N. Integrating bulk and single-cell transcriptomics with machine learning reveals a heme metabolism-based panel for lung adenocarcinoma chemotherapy resistance. Int J Mol Sci. 2025; 26(10):4685. https://doi.org/10.3390/ijms26104685 PMID: 40429829 PMCID: PMC12112545.
75. Yao N, Han L, Sun H, Zhou L, Wei Z. Androgen receptor expression and clinical significance in breast cancer. World J Surg Oncol. 2025; 23(1):48. https://doi.org/10.1186/s12957-025-03673-w PMID: 39934842 PMCID: PMC11816761.
76. Yuan J, Chen TT, Chen XC, Ning Y, Tao X, Gu WY. Primary ovarian mesonephric-like adenocarcinoma: a clinicopathological analysis of 17 cases. Zhonghua Bing Li Xue Za Zhi. 2025; 54(5):494-499. https://doi.org/10.3760/cma.j.cn112151-20241113-00752 PMID: 40302579.
77. Zou S, Zhang L, Jiang C, Li F, Yang Y, Deng X, Zhang J, Chen H, Jiang L, Cheng X, Deng L, Lin L, Shen B, Wen C, Zhan Q. Driver mutation subtypes involve with differentiated immunophenotypes influencing pancreatic cancer outcomes. Cancer Lett. 2024; 599:217134. https://doi.org/10.1016/j.canlet.2024.217134 PMID: 39094824.
78. Torres-Ruiz S, Garrido-Cano I, Lameirinhas A, Burgués O, Hernando C, Martínez MT, Rojo F, Bermejo B, Tapia M, Carbonell-Asins JA, Peña CJ, Lluch A, Cejalvo JM, Tormo E, Eroles P. MiRNA-449 family is epigenetically repressed and sensitizes to doxorubicin through ACSL4 downregulation in triple-negative breast cancer. Cell Death Discov. 2024; 10(1):372. https://doi.org/10.1038/s41420-024-02128-7 PMID: 39174500 PMCID: PMC11341569.
79. Chaudhry GE, Md Akim A, Sung YY, Sifzizul TMT. Cancer and apoptosis: the apoptotic activity of plant and marine natural products and their potential as targeted cancer therapeutics. Front Pharmacol. 2022; 13:842376. https://doi.org/10.3389/fphar.2022.842376 PMID: 36034846 PMCID: PMC9399632.
80. Langelier MF, Planck JL, Roy S, Pascal JM. Structural basis for DNA damage-dependent poly(ADP-ribosyl)ation by human PARP-1. Science. 2012; 336(6082):728-732. https://doi.org/10.1126/science.1216338 PMID: 22582261 PMCID: PMC3532513.
81. Tandon A, Sinha S. Structural insights into the binding of MMP9 inhibitors. Bioinformation. 2011; 5(8):310-314. https://doi.org/10.6026/97320630005310 PMID: 21383916 PMCID: PMC3046033.
82. Li Y, Wang F, Chen X, Wang J, Zhao Y, Li Y, He B. Zinc-dependent deacetylase (HDAC) inhibitors with different zinc binding groups. Curr Top Med Chem. 2019; 19(3):223-241. https://doi.org/10.2174/1568026619666190122144949 PMID: 30674261.
83. Read ML, Brookes K, Zha L, Manivannan S, Kim J, Kocbiyik M, Fletcher A, Gorvin CM, Firth G, Fruhwirth GO, Nicola JP, Jhiang S, Ringel MD, Campbell MJ, Sunassee K, Blower PJ, Boelaert K, Nieto HR, Smith VE, McCabe CJ. Combined

vorinostat and chloroquine inhibit sodium-iodide symporter endocytosis and enhance radionuclide uptake *in vivo*. Clin Cancer Res. 2024; 30(7):1352-1366. https://doi.org/10.1158/1078-0432.CCR-23-2043 PMID: 37921808 PMCID: PMC7615786.

84. Clark JJ, Benson ML, Smith RD, Carlson HA. Inherent versus induced protein flexibility: comparisons within and between apo and holo structures. PLoS Comput Biol. 2019; 15(1):e1006705. https://doi.org/10.1371/journal.pcbi.1006705 PMID: 30699115 PMCID: PMC6370239.
85. Liu K, Kokubo H. Exploring the stability of ligand binding modes to proteins by molecular dynamics simulations: a cross-docking study. J Chem Inf Model. 2017; 57(10):2514-2522. https://doi.org/10.1021/acs.jcim.7b00412 PMID: 28902511.
86. Shokoohinia Y, Gheibi S, Kiani A, Sadrjavadi K, Nowroozi A, Shahlaei M. Multi-spectroscopic and molecular modeling investigation of the interactions between prantschimgin and matrix metalloproteinase 9 (MMP9). Luminescence. 2016; 31(2):587-593. https://doi.org/10.1002/bio.2999 PMID: 26311532.
87. Mathpal S, Sharma P, Joshi T, Pande V, Mahmud S, Jeong MK, Obaidullah AJ, Chandra S, Kim B. Identification of zinc-binding inhibitors of matrix metalloproteinase-9 to prevent cancer through deep learning and molecular dynamics simulation approach. Front Mol Biosci. 2022; 9:857430. https://doi.org/10.3389/fmolb.2022.857430 PMID: 35463960 PMCID: PMC9024349.
88. Laronha H, Caldeira J. Structure and function of human matrix metalloproteinases. Cells. 2020; 9(5):1076. https://doi.org/10.3390/cells9051076 PMID: 32357580 PMCID: PMC7290392.

Author Contribution

NG designed the experimental protocol and supervised the study. NG and KR conducted the study and drafted the manuscript. NG reviewed and finalised the manuscript. All authors have read and agreed to the published version of the manuscript.